# Transport of sediments in numerical simulation of sedimentary basins


Carlos Vitor A. Carvalho

*Tecgraf/PUC-Rio – Computer Graphics Technology Group*
*PUC-Rio – Pontifical Catholic University of Rio de Janeiro*

Luiz Fernando Martha

*Civil Engineering Department and Tecgraf/PUC-Rio*
*PUC-Rio – Pontifical Catholic University of Rio de Janeiro*

Eurípedes do Amaral Vargas Júnior

*Civil Engineering Department*
*PUC-Rio – Pontifical Catholic University of Rio de Janeiro*



## *Abstract*

*This paper describes an algorithm for transport of sediments in a 3D numerical simulation of depositional processes in platform, slope, and basin environments. The algorithm is based on quantitative concepts of Sequence Stratigraphy, as primary control mechanisms of the sedimentary strata architecture, and on a 2D, steady-state, Navier-Stokes flow. The objective of this simplified analysis, which is performed in each step of the sedimentation simulation, is to obtain a velocity field distribution within the simulation area, which is represented by a regular grid. The velocity field is calculated from boundary conditions along the cross-shore (sediment aport velocity) and long-shore directions (field stream velocity), and from the bathymetry of the region. The velocity field is used to calculate, by means of a Runge-Kutta interpolation method, stream-lines that determine the direction of sediment transport.*


## 1 INTRODUCTION

Sedimentary Geology deals with the physical, chemical and biological processes that affect the formation of sedimentary rocks. One of its main focuses lies in the determination of parameters and processes that control the in-fill of sedimentary basins. For this, the development of a geologic model is necessary (Popp, 1998).

A geologic model may be classified according to the parameters and processes that are considered in its representation (Figure 1):

- **Conceptual model**: theoretical, based on premises and qualitative descriptions;
- **Interpretative** model: based on the correlation of data and space association;
- **Physical model**: based on an experimental or physical simulation;
- **Mathematical model**: based on mathematical/numerical algorithms.

In simple cases, the use and formulation of an interpretative or conceptual model might be sufficient. However, for situations that require synchronous or quantitative answers, the benefits of numerical modeling in general justify its use in spite of its intrinsic complexity.

Numerical geologic modeling adopts two distinct approaches (Figure 2). In the first, called forward modeling, the simulation of the evolution of a sedimentary basin is performed from the past to the present days. The initial conditions are defined by a group of parameters and specified processes. The objective of the simulation is to obtain a final sedimentary architecture, which is then compared to the interpretative model.

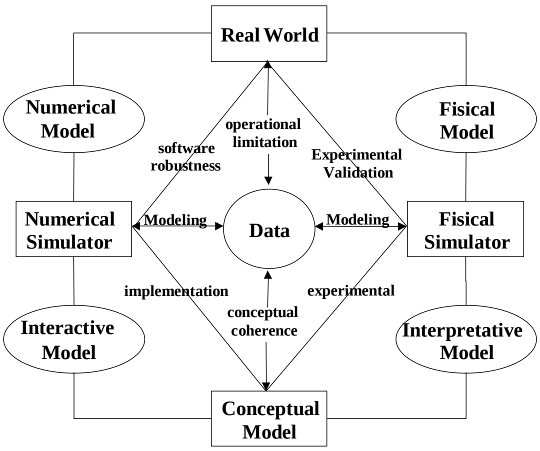


Figure 1 – Types of geologic models and involved processes. Adapted from Faccion (2002).

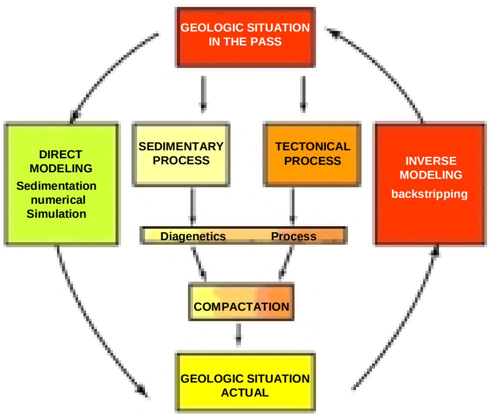


Figure 2 – Classification of the Programs of Numeric Simulation in Geology with relationship to the sense of Modeling. Adapted from Faccion (2002).

In the second approach, called backward modeling, the objective is to find the parameters and processes that determine the current sedimentary architecture, which is based on data interpretation. In the latter case, the processes and parameters are obtained using, for example, backstripping or restoration techniques (Tearpock & Bischke, 1991; Ferraz, 1993, Santi, 2002).

The simulation performed in this work is in the direct modeling group. The simulation is based on quantitative concepts of Sequence Stratigraphy, as primary control mechanisms of the sedimentary strata architecture, and on a fluid flow numerical analysis for sediment transport.

Figure 3 shows the main stages of the algorithm developed in present simulation for transport and deposition of siliciclastic sediments. The focus of this paper is the algorithm of sediment transport in the formation of sedimentary basins. As a goal, this algorithm should consider the following aspects:

- Varying aport of sediment supply along the shore line;
- Influence of sea bottom bathymetry (platform slope, canyons, etc.) in sediment transport;
- Cross-shore currents.

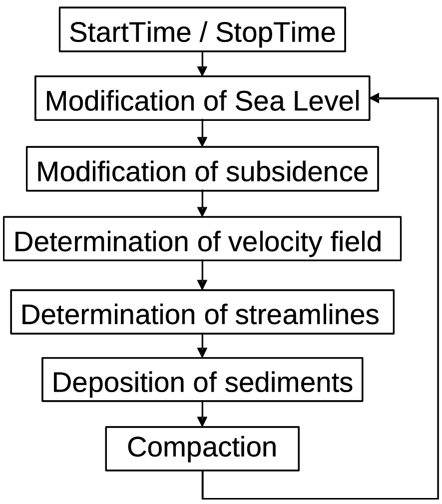


Figure 3 – Main stages of present sedimentation simulation.

### 1.1 Geologic processes used in the simulation

According to Vail (1987), the main processes that control the patterns of strata and distributions of lithologies facies in sedimentary basins are (Figure 4): tectonic subsidence, variation of the sea level (eustatic curve), and sediment supply.

The accommodation, that is, the available space for potential accumulation of sediments in the basin, is function of the eustatic variation and subsidence (Fig. 5).

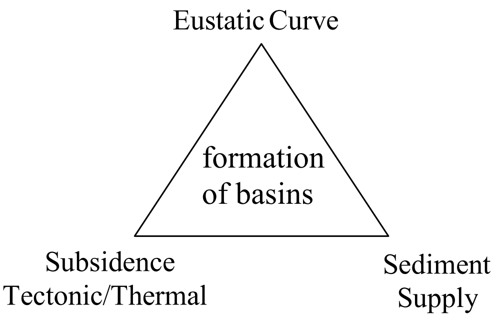


Figure 4 – Geologic processes responsible for the formation of sedimentary basins.

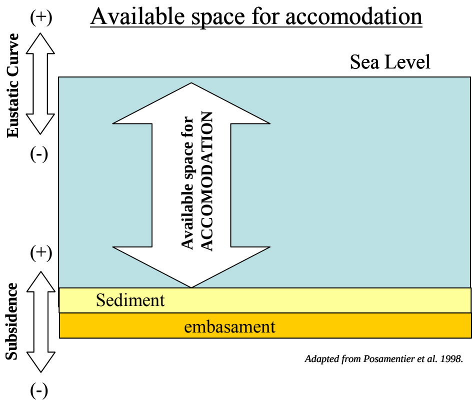


Figure 5 – Available space generated by the relation between sea level variation and subsidence. Adapted from Posamentier et al. (1998).

With the parameters and geologic processes defined, the next stage in the simulation is to determine the velocity field that will be used to transport the sediments. This is described in the next sections.

## 2 FORMULATION

This work adopts a hydrodynamic approach for sediment transport that simplifies the actual fluid flow in the real phenomenon. Rather, a net distribution of velocities is considered in each time step of the sedimentation simulation.

The derivation of the fluid flow equations, in the context of this work, considers an elementary area inside the mass of a fluid in movement, with forces acting at opposite faces, as shown in Figure 6.

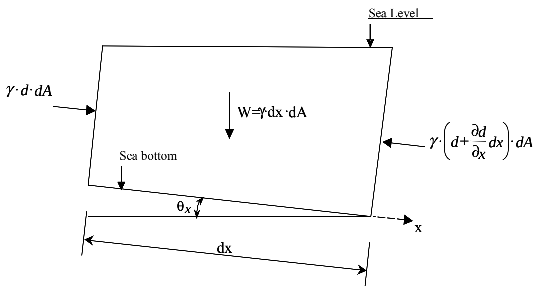


Figure 6 – Elementary area for the derivation of fluid flow equations.

In a general case, the governing fluid flow equations (Navier-Stokes) are defined according to the following types of physics assumptions:

- Conservation of mass (continuity equation);
- Newton's second law (momentum conservation);
- Energy conservation.

In the present simplified approach, a 2D fluid flow analysis is considered, assuming that the transport of sediments will just be made in the directions *x* and *y* (cross-shore and long-shore directions, respectively). That is, it is assumed that the velocity field at each point does not vary along the vertical $z$ direction. Since temperature variation in not considered in this simplified analysis, energy conservation equations are not used in the formulation of the problem. An incompressible and non-viscous fluid flow is admitted.

With the simplifications described above and using the elementary area of Figure 6, conservation of mass results in the following continuity equation, where $d$ is the water depth, and $u$ and $v$ are the components of the velocity vector in the directions $x$ and $y$, respectively.

$$\frac{\partial u}{\partial x}+\frac{\partial v}{\partial y}=-\frac{1}{d}\left(u\frac{\partial d}{\partial x}+v\frac{\partial d}{\partial y}\right) \quad (1)$$

Newton's second law results in the following momentum conservation equations in directions $x$ and $y$, respectively, where $\sin\theta_x$ and $\sin\theta_y$ are the inclinations of the sea bottom in each direction:

$$\frac{\partial d}{\partial x}+\sin\theta_x+\frac{u}{g}\cdot\frac{\partial u}{\partial x}+\frac{v}{g}\cdot\frac{\partial u}{\partial y}=0 \quad (2)$$

$$\frac{\partial d}{\partial y}+\sin\theta_y+\frac{u}{g}\cdot\frac{\partial v}{\partial x}+\frac{v}{g}\cdot\frac{\partial v}{\partial y}=0 \quad (3)$$

## 2.1 Fluid flow analysis

Combining eqs. (1), (2), and (3) results in eq., (4), which is a Poisson type differential equation written in Cartesian coordinates (Fortuna, 2000; Carvalho, 2003):

$$\frac{\partial^2\phi}{\partial x^2}+\frac{\partial^2\phi}{\partial y^2}=f(x,y) \quad (4)$$

In eq. (4), $f(x,y)$ is the sea bottom bathymetry and $\phi$ is the flow velocity potential:

$$u=\frac{\partial\phi}{\partial x} \quad (5)$$

$$v=\frac{\partial\phi}{\partial y} \quad (6)$$

Eq. (4) is discretized using the Finite Difference Method, in which differential terms are substituted by difference terms as follows:

$$\begin{aligned}&\left(\phi_{i,j+1}-2\phi_{i,j}+\phi_{i,j}-u\Delta x\right)\cdot(\Delta y)^2+\\&\left(\phi_{i-1,j}-2\phi_{i,j}+\phi_{i+1,j}\right)\cdot(\Delta x)^2=\\&(\Delta x)^2(\Delta y)^2 f(x_i,y_j)\end{aligned} \quad (7)$$

Similarly, the finite difference versions of eqs. (5) and (6) may be written as:

$$u=\frac{\partial\phi}{\partial x}\cong\frac{\phi_{i,j}-\phi_{i,j-1}}{\Delta x} \quad (8)$$

$$v=\frac{\partial\phi}{\partial y}\cong\frac{\phi_{i,j}-\phi_{i-1,j}}{\Delta y} \quad (9)$$

In this finite difference approach, gradients are computed using the nodal grouping shown in Figure 7.

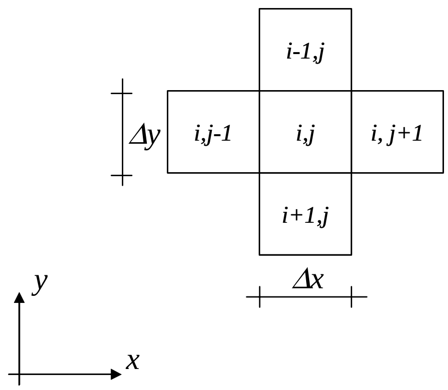


Figure 7 – Nodal grouping used in the finite difference discretization.

The solution to this type of Boundary Value Problem (BVP) is obtained specifying conditions of the dependent variable at the border $\delta R$ of the simulation area $R$.

It is important to observe that, in this work, the boundary conditions are not defined in terms of velocity potential. Rather they are defined in the form of a velocity vector at each boundary cell of the discretized area.

The formulation of the discrete eq. (7) for each cell of the grid, also considering boundary conditions, results in a system of equations, whose coefficients form a symmetric pentadiagonal matrix. It has five bands, and contains a band of zeros between the two off-diagonal non-zero bands on either side.

The solution of this equation system may be obtained by iterative or direct methods. In direct methods, the zero bands must be included in the calculations and they will fill with non-zero numbers during the matrix decomposition. With large matrices, this procedure may become costly. Iterative methods, on the other hand, may be programmed to skip the zero terms. Details on those methods can be seen in Fortuna (2000).

In the present work, the system of equations is solved using a Gauss-Seidel iterative method, resulting in the velocity potential in all the cells of the grid. Using relationships (8) and (9), the components of the velocity vector are computed in each cell.

Figure 8 and 9 show an example of the implemented strategy. This example consists of a region with a varying bathymetry, with an imposed parallel boundary velocity field (Figure 8). Figure 9 shows the velocity field obtained by the steady-state fluid flow analysis.

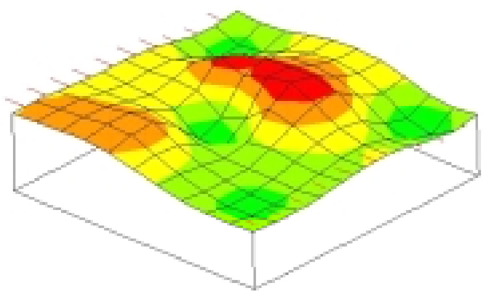

Figure 8 – Bathymetry contours and parallel boundary velocity field.

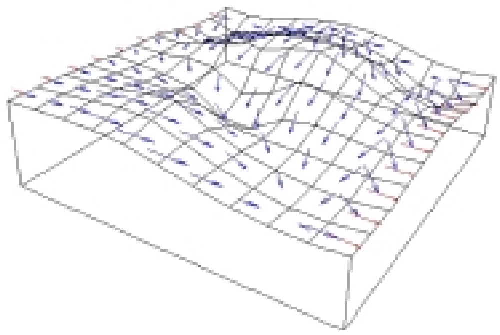

Figure 9 – Computed velocity field of example of Figure 8.

## 2.2 Streamline computation

In the present sedimentation simulation strategy (Figure 3), after computing the velocity field, it is necessary to evaluate the trajectories inside the grid through which the sediments will be transported. In the visualization and analysis of fluid flow, it is common to evaluate those trajectories as streamlines (Martinez, 1995). Streamlines are, in an instant of time, tangent at all points to the velocities. Each streamline has the same velocity potential.

The determination of streamlines in the present simulation consists of solving an Initial Value Problem (IVP), in which the initial value of each streamline is a point $(x, y)$ at the shore border of the simulation area, as shown the Figure 10. This initial point $(x, y)$ is associated to a velocity vector that corresponds to the input boundary cross-shore velocity used in the flow analysis.

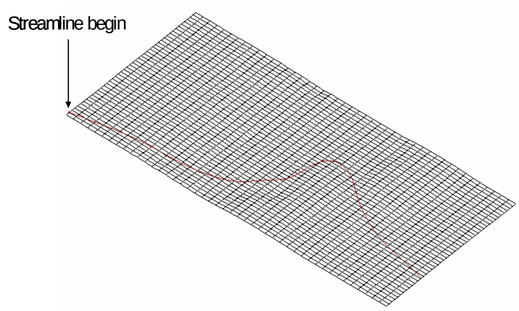


Figure 10 – Streamline starting at a point at the shore border.

Several numerical methods exist to determine streamline trajectories (Boyce, 1992). This work uses a Runge-Kutta interpolation method of the fourth order proposed by Royer (2001). This method combines accuracy, simplicity and is easy to implement. The errors are of $O(h^5)$, where $h$ is the step size.

In this work, the IVP streamline problem may be formulated as: given a known streamline point $(x_n, y_n)$, the objective is to calculate the position $(x_{n+1}, y_{n+1})$ of the next point. This results in the following expressions:

$$x_{n+1} = x_n + \frac{h}{6}\left[k1(x,y) + 2\cdot k2(x,y) + 2\cdot k3(x,y) + k4(x,y)\right] \quad (10)$$

$$y_{n+1} = y_n + \frac{h}{6}\left[m1(x,y) + 2\cdot m2(x,y) + 2\cdot m3(x,y) + m4(x,y)\right] \quad (11)$$

where:

$k1(x,y) = u(x,y)$ is the value of component $x$ of the velocity vector;
$m1(x,y) = v(x,y)$ is the value of component $y$ of the velocity vector,

The other factors are:

$$k2(x,y) = u\left(x + \frac{h}{2}k1(x,y), y + \frac{h}{2}m1(x,y)\right)$$

$$m2(x,y) = v\left(x + \frac{h}{2}k1(x,y), y + \frac{h}{2}m1(x,y)\right)$$

$$k3(x,y) = u\left(x + \frac{h}{2}k2(x,y), y + \frac{h}{2}m2(x,y)\right)$$

$$m3(x,y) = v\left(x + \frac{h}{2}k2(x,y), y + \frac{h}{2}m2(x,y)\right)$$

$$k4(x,y) = u\left(x + \frac{h}{2}k3(x,y), y + \frac{h}{2}m3(x,y)\right)$$

$$m4(x,y) = v\left(x + \frac{h}{2}k3(x,y), y + \frac{h}{2}m3(x,y)\right) \quad (12)$$

The values $u(x,y)$ and $v(x,y)$ are calculate using a bilinear interpolation. Considering a cell of the grid that has a scalar property $\alpha$ defined at each vertex, the bilinear interpolation of this property at any location inside of the cell is defined as a combination of four bilinear coefficients according to the expression:

$$\alpha = \sum_{i=0}^{3} b[i]\cdot\alpha_i \quad (13)$$

where $b[i]$ are the bilinear coefficients of the vertices of a cell. For a pair of parametric coordinates $(\xi,\eta)$ (Figure 11) of the evaluation point, the values of the bilinear coefficients are:

$$\begin{aligned} (0,0)&\rightarrow & b[0] &= (1-\xi)\cdot(1-\eta) \\ (1,0)&\rightarrow & b[1] &= \xi\cdot(1-\eta) \\ (0,1)&\rightarrow & b[2] &= (1-\xi)\cdot\eta \\ (1,1)&\rightarrow & b[3] &= \xi\cdot\eta \end{aligned} \quad (14)$$

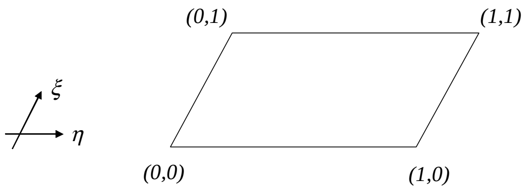


Figure 11 – Parametric coordinates of the vertices of a cell used for the bilinear interpolation.

Figure 12 shows streamlines that were computed by the method described in this section for the example shown in Figures 8 and 9.

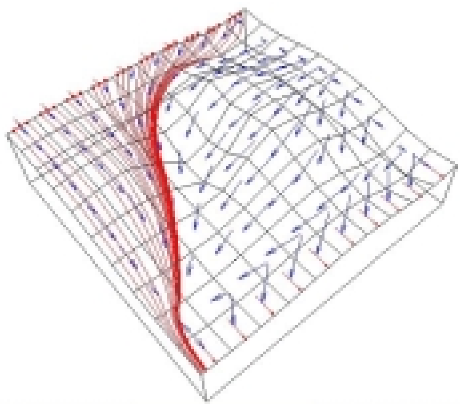

Figure 12 – Streamlines of the example of Figures 8 and 9.

## 2.3 Sediment deposition

The next step in the present sedimentation simulation (Figure 3) is the transport and deposition of sediments. In the transport and deposition of sediments along the streamlines, it was considered that each streamline receives a volume fraction of the total discharge of sediments. That fraction is divided according to three grain sizes: sand, silt and clay. With the volumes of each of them defined for each streamline, the transport / deposition process can be initiated.

During this process, particles travel along the streamlines, starting from the shore border where the sediment is supplied. Each streamline is defined by a set of points. At each point, there is an attempt to deposit each lithologic fraction coming along the streamline. Deposition depends not only on available space but also on the bottom bathymetry gradient. To take this into account, it is admitted that the streamline also follows the bottom bathymetry gradient. This gradient is compared to a stability angle for deposition of each lithologic fraction (sand, silt and clay) (Carvalho, 2002).

# 3 EXAMPLES

Figures 13, 14, and 15 show three models with streamlines computed by the method described in the previous section. One may observe that the streamlines follow the low bathymetry of the simulation area. In the figures, the map of colors indicates the bathymetry: hot (dark) colors show high bathymetry values and cold (light) colors show low bathymetry values.

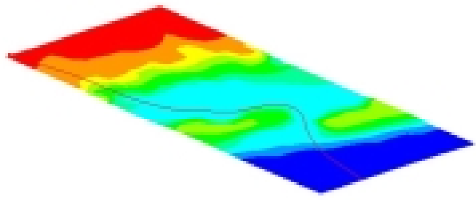

Figure 13 – Example A: bathymetric contour and a streamline of a model with dimensions 100km x 300 km.

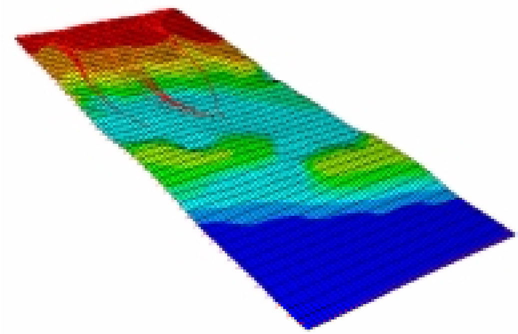

Figure 14 – Example B: bathymetric contour and a set of streamlines of a model with dimensions 100km x 300 km.

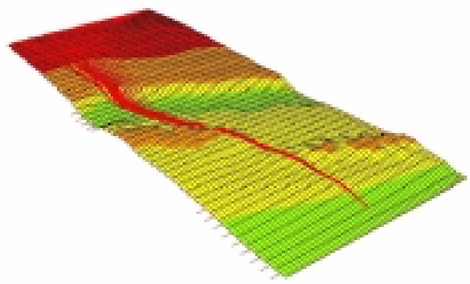

Figure 15 – Example C: bathymetric contour and a set of streamlines of a model with dimensions 100km x 300 km.

Figure 16 shows an example of the sedimentation process in an area of 100 km along the coast line and 250 km basinwards. The bathymetry of this area was modified to simulate platform, slope and deep basin environments and to emphasize some canyons at the border the platform, one of them related to the occurrence of a river represented by a high value of sediment supply at the shore border. Contourite currents at the base of continental slope and the occurrence of salt domes are also simulated in this example. Time span of simulation was of 25 million years. The simulation was divided into 8 steps. Figure 17 shows the streamlines in the first step. Figures 18, 19, 20, and 21 show the deposition of sediment at the end of some steps of the simulation.

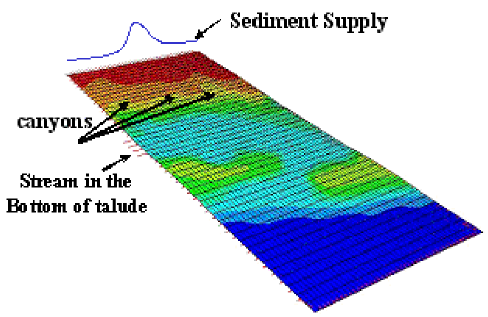


Figure 16 – Example D: bathymetric and characteristic of the model.

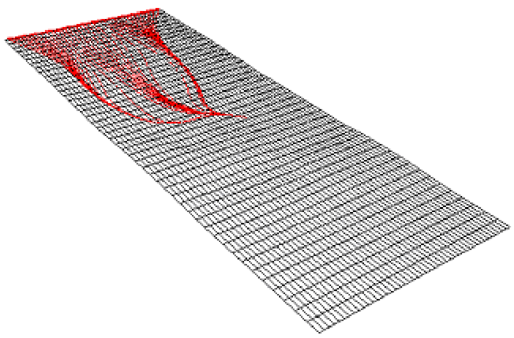

Figure 17 – Streamlines of the first step of simulation.

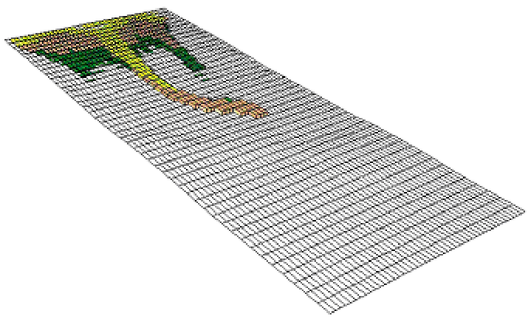

Figure 18 – Deposition at the end of first step.

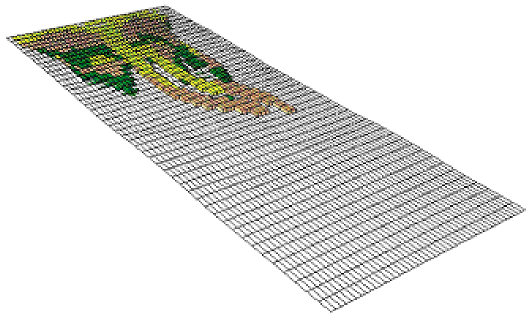

Figure 19 – Deposition at the end of second step.

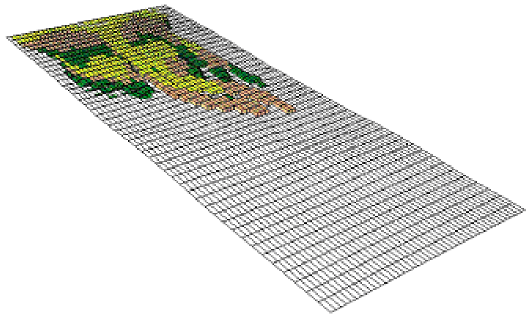

Figure 20 – Deposition at the end of third step.

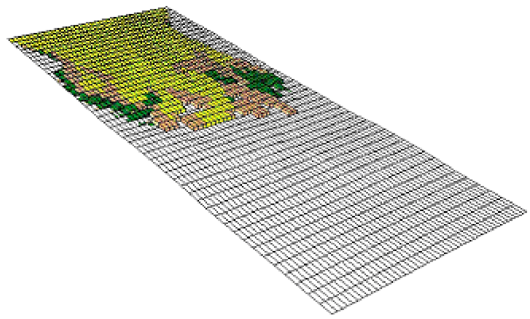

Figure 21 – Deposition at the end of simulation.

## 4 CONCLUSIONS

This paper describes an algorithm for the transport of sediments in a simulation of formation of sedimentary basins. The algorithm considerers a net steady-state Navier-Stokes fluid flow in each step of simulation. In addition, it assumes a two-dimensional fluid flow in which the velocity is constant along the water depth.

The idea of this simulation is not to reproduce the actual physical phenomenon. Instead, the adopted approach tries to incorporate in the simulation the main global parameters that govern the sedimentation problem in the stratigraphic scale: sediment aport, subsidence and sea level variation. The simplified fluid flow analysis for sediment transport is consistent with the type and time scale of the simulation.

Boundary conditions consist of longshore and cross-shore transport velocities. Sediment transport is performed with the aid of streamlines that are generated in each step of the simulation. It was observed that the streamlines accompany the flow according to imposed boundary conditions and to the bathymetry of the sea bottom.

Therefore, the present algorithm was successful in considering non-uniform sediment supply along the shore line, the influence of sea bottom bathymetry in sediment transport, and cross-shore currents.

REFERENCES

Carvalho C. V. A. (2002), “Simulation of transport and deposition of siliciclastic sediments in plataform, slope, and basin environments", Ph.D. Thesis (in Portuguese), Departament of Civil Engineering, PUC-Rio.

Faccion J. C .(2002), “Internal Report Cenpes/PETROBRAS” (in Portuguese), Rio de Janeiro.

Ferraz M.F.R. (1993), “Restoration of Geological Cross-sections Using Planar Subdivisions, Geometric Transformations and Interactive Computer Graphics”. M.Sc. Dissertation (in Portuguese), Department of Computer Science, PUC-Rio.

Fortuna A. O. (2000), “Computational Techniques for Fluids Dynamics”, (in Portuguese), Ed USP.

Martinez, M. L., Zuffo, J.A. (1995), “Use of Streamlines, Pathlines and Streaklines in Flow Visualization”, (in Portuguese) (SIBGRAPI'95). São Carlos-SP-Brasil, pg.303-304.

Posamentier H. W. & Vail, P. R (1988), “Eustatic Control on clastic deposition II – Sequences and systems tracts models”, In: Wilgus, C.K.;Hastings, B.S.; Kendal, C.G.S.C.; “Sea-Level Changes – an Integrated Approach.”, Tulsa, SEPM, p. 125-154, (SEPM sp. Pd. #42).

Popp J. H. (1988), “General Geology” (in Portuguese), LTC, São Paulo.

Royer J. J., Voillemont J. C. (2001), “Building 3D streamlines in GOCAD”, 21st GOCAD – Meeting.

Santi M.R. (2002), Computational Procedures for Restoration of Geological Cross-sections. Ph.D. Thesis (in Portuguese), Department of Civil Engineering, PUC-Rio.

Tearpock, D.J.; Bischke, R.E. (1991), *Applied Subsurface Geological Mapping*. Publisher: Pearson Professional Education. New Jersey – USA.